Analysis of the function of periostin isoform 3 in bladder cancer development and progression

Student's Name: Zhansaya Torebayeva

PI: Eva Riethmacher

Co-PI: Dieter Riethmacher

Date: March 1, 2026

Abstract.

Bladder cancer takes up the eighth place among the most commonly diagnosed cancers worldwide, as in 2020, there were 573 278 incident cases, with 212 536 deaths documented. Bladder cancer primarily affects individuals over 60 and it is more prevalent in men than women. Despite a variety of existing treatments, high recurrence rate and progression to severe forms prove the need for novel solutions. The tumor microenvironment, comprising non-tumor cells and extracellular matrix proteins (ECM), plays a crucial role in cancer development. Periostin, an ECM protein known for its function in cell adhesion and structural maintenance, was shown to be overexpressed in cancer cells. It was associated with tumor formation in breast, lung and colon cancers. This study focused on expression of its isoform 3, and analyzed its function in proliferation of urinary bladder cancer cells. Growth in the number of MB49 2C9 cells, where the periostin gene was knocked out, was compared with MB49 2C9 cells expressing transcript variant 3. Both groups demonstrated time-dependent increase in cell count and fold change over a 72-hour period. No statistically significant difference was found between proliferation of two groups, implying that isoform 3 did not have proliferative effect in given experimental conditions.

Introduction.

Urinary bladder cancer is the eighth most commonly diagnosed cancer in the world, with 212 536 deaths reported in 2020 (Sung et al., 2021). The majority of cases are diagnosed in people over 55, men having four-fold higher likelihood than women. Urothelial bladder cancer, 90% of all cases, can proliferate beyond urothelium and metastasize to distant organs, while squamous cell bladder carcinoma (5% of cases), is associated with schistosomiasis, and rarer types make up the remaining 5% (Saginala et al., 2020). Transurethral resection with immunotherapy and

radical cystectomy with neoadjuvant chemotherapy are two treatment choices for non-muscle-invasive bladder cancer (NMIBC) and muscle-invasive type (MIBC) respectively (Babjuk et al., 2022). Despite advancing treatment, therapeutic options stay limited, which demonstrates a growing need for early detection biomarkers to understand tumor progression better.

Cancer progression depends on extracellular matrix proteins (ECM) that constitute the tumor microenvironment (Murphy and Sage, 2014). Periostin, encoded by the gene *POSTN*, is an ECM matricellular protein, whose main function is to form structural support and maintenance in bones, tendons, ligaments and heart valves (Silvers et al, 2016). Interaction of periostin with other cells happens through its four FAS1 domains, while connection with ECM proteins occurs through EMI domain, both found in the N-terminal region (Litvin et al, 2004). Periostin's binding with integrins results in cell adhesion and cell spreading (Ruan et al., 2009). The C-terminal region of the protein interacts with fibronectin, collagen, tenascin C, heparin and periostin itself (Morra and Moch, 2011).

Recent studies highlighted periostin's function in tumor development, as it showed high expression in different tumors like pancreatic, ovarian, colon, along with breast cancer (Morra and Moch, 2011). While Kim et al. (2005) demonstrated that high-grade bladder cancer expressed less periostin mRNA, more recent studies described elevated levels of periostin mRNA in high-grade MIBC, together with lower levels of the protein in low-grade NMIBC (Silvers et al., 2016).

Upon exposure to alternative splicing, new isoforms of periostin are formed, resulting in diverse characteristics. Ten different human isoforms, besides a full-length variant, are

known currently (Dorafshan et al, 2022). Since periostin isoforms illustrate varied invasiveness, it is under investigation, how isoform-specific connection with ECM affects its proliferative abilities (Morra and Moch, 2011). In this project, proliferative effect of isoform 3, characterized by absence of exons 17 and 21, will be analyzed by comparing growth of the cells with isoform 3 with the knock-out cells.

Methods.

To analyze the proliferative function of periostin isoform 3, cell proliferation assay by direct cell counting was performed.

Cell lines.

The cell line that was used for this experiment was MB49 2C9 cells, a model transitional cell carcinoma derived from C57BL/6 mice was used in this experiment. MB49 2C9 knockout cells were taken as control, while MB49 2C9 cells with Transcript variant 3 were taken as transfected cells. In order to achieve the gene knockout, CRISPR-Cas9 genome editing technology was used. The guide RNAs targeting the gene of interest (*POSTN*) were designed and were introduced into MB49 2C9 cells together with Cas9 nuclease to induce site-specific double-strand breaks. Then, clonal selection and validation of knockout efficiency were confirmed. To achieve selective expression of isoform 3, cells were transfected with a plasmid encoding isoform 3 only. Transfection was carried out using Lipofectamine reagent in accordance with the provided protocol. All transfection procedures were conducted by Anton Borrissenko.

Growing of cells.

These cells were maintained in standard DMEM medium with 10% FBS (Fetal Bovine Serum), 1% NEAA (Non-Essential Amino Acids) and 1% PenStrep (Penicillin-Streptomycin) supplements and incubated in 10 cm petri dishes in 10 mL media at 37°C, with 5% CO_2. For maintenance, when the cells reached 90% confluence, they were split into new 10 cm wells to prevent overgrowth. The cells at the same level of confluency were used for the experiments.

Splitting the cells.

For splitting, first, the cells were observed under a microscope to check for confluency. Then, the culture medium was aspirated, and cells were washed with sterile phosphate-buffered saline (PBS) two times to remove residual parts. 2 mL of 0.05% trypsin–EDTA was added to cover the cells in 10-cm plate and they were incubated at 37 °C for 1,5-2 minutes until cells detached. Detachment was confirmed and facilitated under the microscope and then trypsin was neutralized by bringing up the volume to the total of 10 mL. Cells were gently washed off the plate and cell suspension was collected in 15 mL falcon tubes. Collected cells were centrifuged at 1000 rpm (revolutions per minute) for 5 minutes, and the pellet was resuspended in 1mL of growth medium. Cells were reseeded at the required density in new 10-cm culture plates for continued growth.

Freezing and thawing process.

For long-term storage, cells were trypsinized and collected as described above, then were added an equal volume of freezing medium containing 10% dimethyl sulfoxide (DMSO) and 90% Fetal Bovine Serum (FBS). Later, they were transferred into cryovials, with aliquotes of $1–3\times10^6$ cells per vial and were placed in freezing container for the first 24 h up to 2 weeks at –80 °C. For longer storage, cells were placed into liquid nitrogen.

In order to defreeze cells, cryovials were first rapidly thawed at room temperature and then the media was transferred to a prewarmed fresh growth medium in a 15 mL falcon tube immediately, in order to minimize DMSO exposure. These were centrifuged at 1000 rpm for 5 minutes; medium was aspirated and 1 mL of new medium was added. Cells were resuspended and seeded in 10-cm culture dishes for continued growth. The culture dishes were gently rocked in perpendicular directions to achieve even spread and were observed under the microscope.

Cell proliferation assay.

For proliferation assay, the growth of cells was assessed by counting the total number of cells at 24 hours, 48 hours, and 72 hours after initial seeding using a hemocytometer. The cells were seeded in a single 6-well plate per experiment, with seeding density of 50 000 cells in 3 mL of medium per well. For each time point 2 adjacent wells were allocated.

First, as preparation before seeding, confluent cells growing in 10-cm petri dishes were trypsinized and collected as was described in the splitting step mentioned above. Then they were manually counted using a hemocytometer. From this value, the number of cells needed, based on the seeding density, was calculated. The calculated number of cells was then transferred to the fresh growth medium in a 50 mL falcon tube to prepare a homogeneous cell suspension, and was mixed thoroughly before being distributed in equal volume into 6 wells. Cells were observed in the microscope after seeding and were maintained in standard culture conditions at 37 °C with 5% CO_2.

For harvesting the cells at each time point, after 24 h, the medium in the first 2 wells was aspirated, washed with 3 mL of PBS two times, and trypsinized with 600 µL of trypsin. Then the cell suspensions were transferred to the falcon tubes and 10 µL aliquot from this suspension was added to each side of the hemocytometer and cells in the central square were counted manually.

Standard hemocytometer protocol was used to calculate the cell concentration. For the next two time points, at 48 hours and 72 hours, the same procedure was repeated and the number of cells was recorded accordingly. Medium was not changed during the process of incubation. This experimental procedure was repeated four times as independent biological replicates, having duplicate wells for each time point in the same 6-well plate. Accordingly, the values from the resulting total of 8 wells per time point were used to make further calculations.

Statistical analysis.

For each time point, cell numbers from two wells in a single 6-well plate were recorded and the average was calculated, to establish one value per biological replicate. The same process was repeated for all four independent replicates, resulting in four average numbers at each time point. The standard deviation (SD) and standard error of the mean (SEM) for each time point were calculated across the four replicates. Fold change was determined relative to the baseline number, which is the seeding density of 50,000 cells. It was calculated by dividing the mean number of cells at each time point by the baseline number.

Statistical analysis between control and transfected cells at each time point was conducted using an unpaired independent two-tailed student's t-test. Average number of duplicate wells were used, so the n for the t-test was equal to the number of replicates. P-value < 0.05 was taken as a statistically significant value for this study. All calculations and statistical tests were done using Microsoft Excel (version 2302). Fold change values were used for visual graphs and comparison only, not for further statistical testing.

Results.

Proliferation of MB49 2C9 cells was assessed over a 72-hour period after seeding. All the recorded data for each time point is given in Table 1. As it can be observed, the control cells showed a time-dependent increase in cell number, rising from a baseline seeding count of 50 000 cells to 117 710 ± 13 335 cells at 24 hours, 617 750 ± 76 328 cells at 48 hours, and 2 221 437 ± 359 885 cells at 72 hours. Growth in cell count is presented as the mean ± standard error of the mean (SEM). These steady increases in cell number reflect 2.35, 12.36, and 44.43-fold increases at each time point, in relation to the baseline respectively (Table 1, Graph 1b). After 24 hours, standard deviation (SD) was found to be 26,669.14, at 48 hours, it rose up to 152 657.84, and at 72 hours, the value was 719 771.04. These values are associated with increased biological variation as the cell density increases. Here, the SD indicates the spread of each biological replicate value around the mean, showing high variability between independent trials. Meanwhile, the SEM shows how precise the estimated mean is among all the replicates.

Figure 1. Proliferation of MB49 2C9 control cells over time.

Table 1.

Time	**Total number of trials**	**Mean number of MB49 2C9 control cells**	**SD**	**SEM**	**Fold change in average number relative to baseline**
0 h seeded	8	50,000			
24 h	8	117710	26669,14	13335	2,35
48 h	8	617750	152657,84	76328	12,36
72 h	8	2221437,5	719771,04	359885	44,43

In the graph 1a, the growth in average number of MB49 2C9 cells at 24 h, 48 h and 72 h after seeding can be observed. The SEM is indicated as error bars in the graph. It can be seen that 72 h cells have the highest SEM and cells had the most growth between 48 h and 72 h.

Graph 1a.

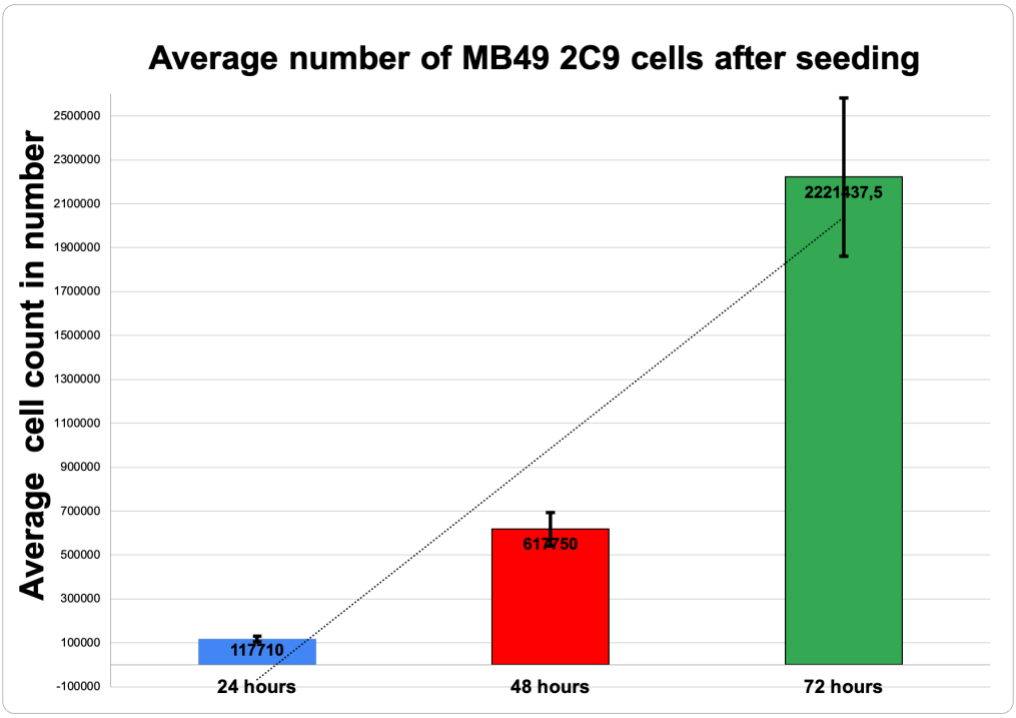

Graph 1b.

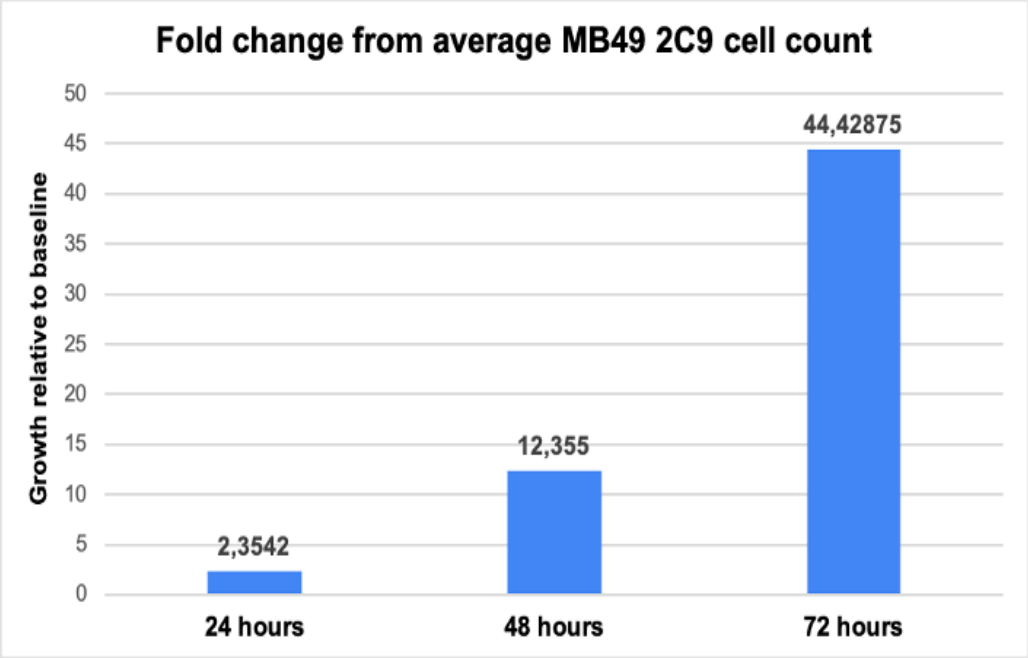

Similar to control cells, MB49 2C9 cells expressing transcript variant 3 illustrated progressive proliferation over a 72-hour period. Mean cell numbers constituted 129 500 ± 16917 at 24 hours, 570 375 ± 39 559 at 48 hours, and 2 192 375 ± 157 352 at 72 hours, presented as the mean ± SEM (Table 2, Graph 2a). There is a higher increase in the number of cells between 48 hours and 72 hours, compared to the first 24 hours or first 48 hours. After 24 hours, SD was found to be 33833,77, at 48 hours it was 79118,45, and at 72 hours, it was 314703,33, showing continuous increase as well. The SD values show an increase in the variability between biological replicates as the incubation time increased. The change in SEM reflects the increase in the dispersion of replicate values as the number of cells increased. The corresponding fold changes for each time point are 2.59, 11.41, and 43.85 times relative to the baseline value respectively (Graph 2b).

Figure 2. Proliferation of MB49 2C9 cells with transcript variant 3 over time.

Table 2.

Time	Number of trials	Mean number of MB49 2C9 cells with Transcript variant 3	SD	SEM	Fold change in average number relative to baseline
0 h seeded	8	50,000			
24h	8	129500	33833,77	16916,88	2,59
48h	8	570375	79118,45	39559,23	11,41
72h	8	2192375	314703,33	157351,67	43,85

In graph 2a, the growth in average number of MB49 2C9 Transcript variant 3 cells at 24 hours, 48 hours and 72 hours after seeding can be seen. The SEM is shown as error bars in the graph.

Graph 2a.

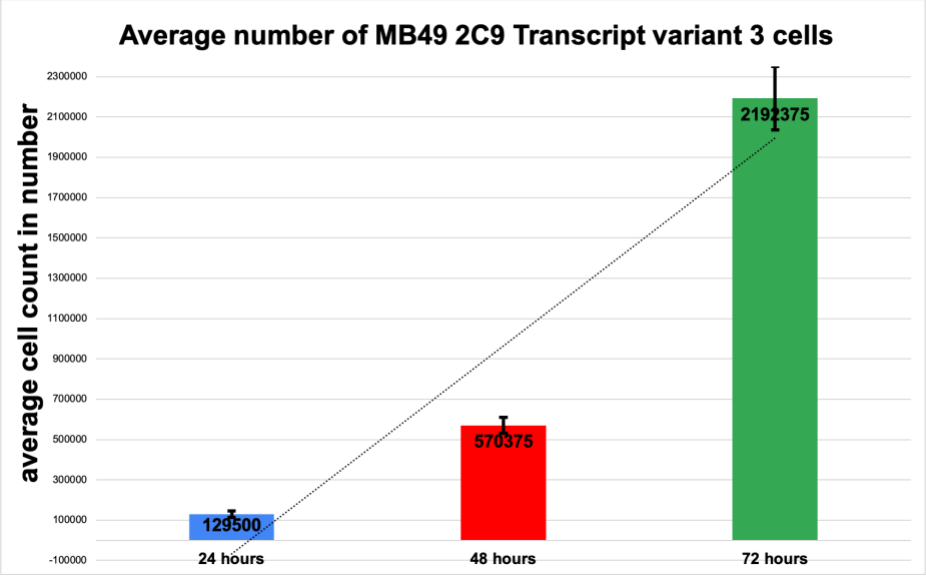

Graph 2b.

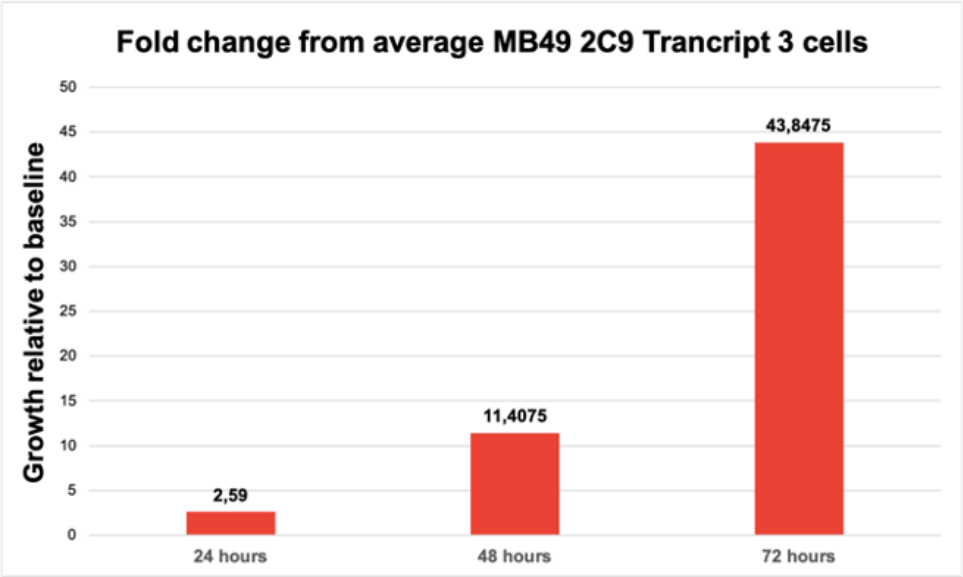

Table 3 shows the comparison in the proliferation number of MB49 2C9 cells between control and transcript variant 3 in the form of mean number of cells ± SD for each time point and each group. An unpaired two-tailed Student's t-test was used to find the statistical difference between the mean values of the knockout cells and transcript variant 3 cells. Direct comparison of cell numbers between control cells and transcript variant 3 containing cells showed no statistical significance at any time point, as p values were 0.444 at 24 hours, 0.436 at 48 hours, and 0.916 at 72 hours (Table 3). All three numbers show a value greater than significance of $p < 0.05$, which demonstrates that there is no notable difference in the growth of these two groups of cells. These findings indicate that expression of isoform 3 did not cause any change in the proliferative capacity of MB49 2C9 cells used in this experiment.

Figure 3. Comparison in proliferation number of MB49 2C9 cells between control and transcript variant 3 at 24 h, 48 h and 72 h after seeding.

Table 3.

Time	**Mean number of MB49 2C9 cells (control) ± SD**	**Mean number of MB49 2C9 cells with Transcript variant 3 ± SD**	**P-value (t-test*)**
24 h	117 710 ± 26 669	129 500 ± 33 833	0,582
48 h	617 750 ± 152 657	570 375 ± 79 118	0,601
72 h	2 221 437,5 ± 719 771	2 192 375 ± 314 703	0,943

Graph 3a compares the average numbers of control MB49 2C9 cells and cells transfected with Transcript variant 3 at 24 hours, 48 hours and 72 hours after seeding. The error bars and number of cells are indicated in the graph. It can be seen that growth of both groups of cells at three different incubation times follow a similar pattern, and values also appear comparable. MB49 2C9 cells have wider error bars at 48 hours and 72 hours, compared to the transfected MB49 2C9 cells. In graph 3b, comparison between fold change numbers in MB49 2C9 cells and cells transfected with Transcript variant 3 can be viewed. Fold changes also demonstrate similar results in both groups, indicating that there was not a significant difference in the growth of the cells.

Graph 3a.

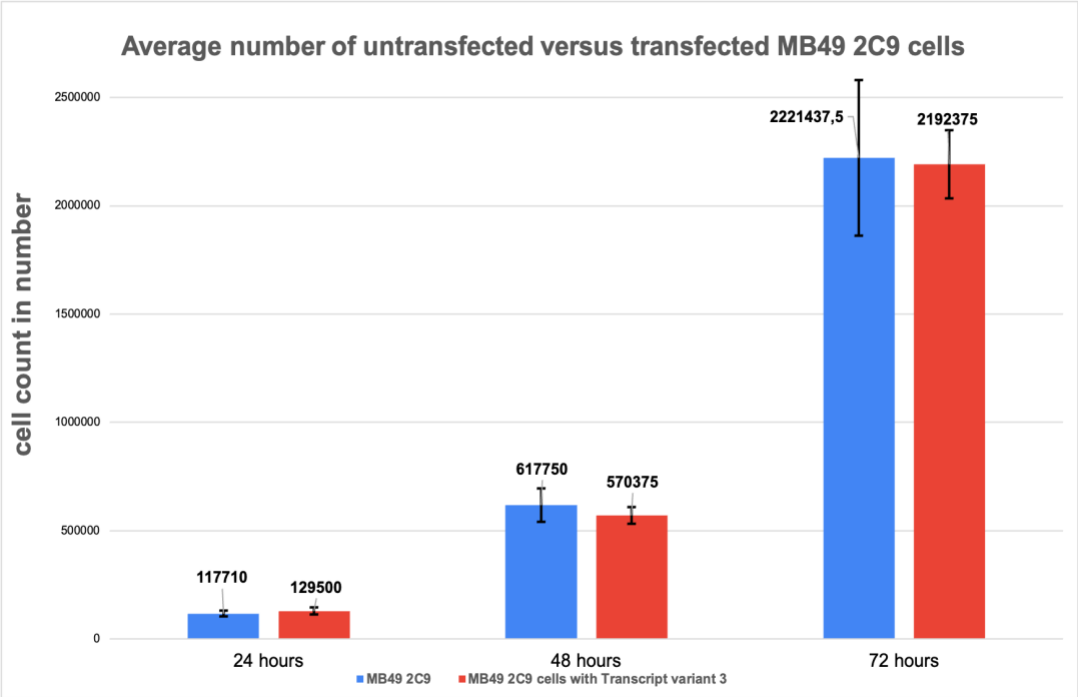

Graph 3b.

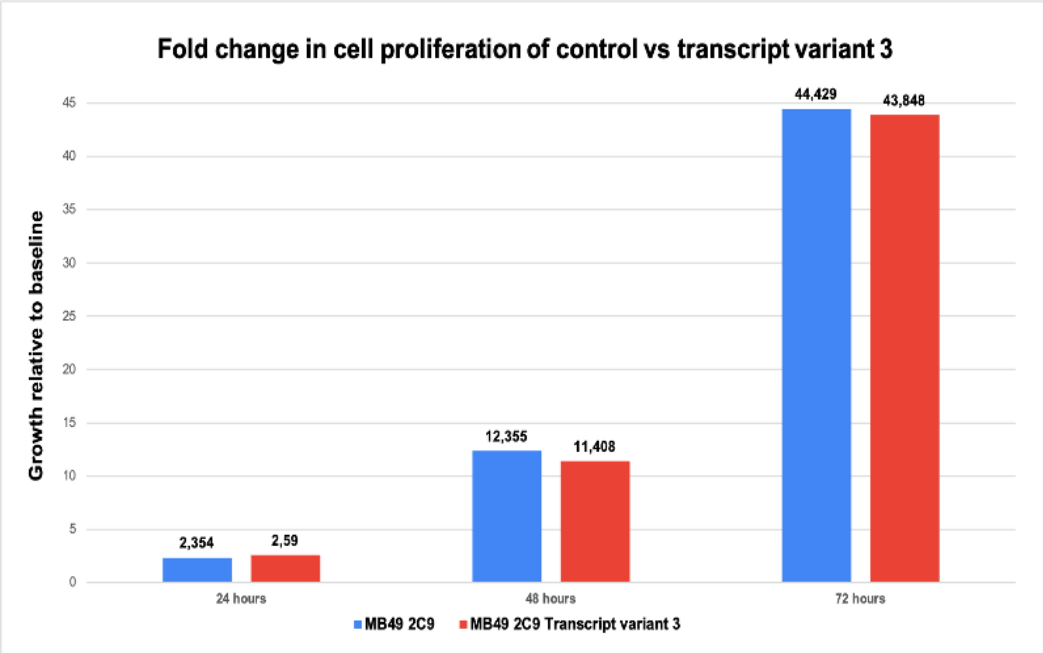

Discussion.

In this study, the effect of isoform 3 of protein periostin expression in MB49 2C9 cell proliferation was assessed using a cell proliferation assay. Both control cells and cells containing isoform 3 displayed a time-dependent increase in cell number over the period of 72 hours, showing an active proliferation under these experimental conditions. However, no statistically significant difference in cell number change was observed between control cells and transcript variant 3 containing cells at all time points. These findings suggest that expression of isoform 3 does not significantly change the proliferative characteristics of MB49 2C9 cells in the given time and conditions analyzed in this study.

It was previously suggested in a number of studies that expression of periostin plays an important role in proliferation of cancer cells. For instance, Xu et al. (2022) reported that POSTN gene knockdown resulted in suppression of proliferation in osteosarcoma and caused activation of PI3K/Akt pathway, while Okazaki et al. (2018) found that in non-small cell lung cancer

periostin promoted proliferation of fibroblast co-culture systems. This may suggest that periostin's proliferative effect is not universal and it might depend on its expression in the certain type of cell or isoform types included. These findings indicate that periostin transcript variant 3 may not promote short-term proliferative capacity of the bladder cancer cells used in this experiment in vitro. Further studies that, for example, include two or more different cell types grown together, along with extracellular matrix components, need to be done to assess the functional role of this periostin isoform more thoroughly in tumor proliferation.

The absence of statistically significant difference between control and transcript variant 3 cells is mostly due to high variability between the biological replicates. Standard deviation numbers increased with the increase of cell number over time, reflecting more dispersion of replicate values at higher density of cells. As a result, the standard error of the mean increased as well. These results offer that even though the mean number of cells were slightly higher in isoform 3 cells, the detected differences were within the range of experimental variability of the study.

References

1. Babjuk, M., Burger, M., Capoun, O., Cohen, D., Compérat, E. M., Escrig, J. L. D., ... & Sylvester, R. J. (2022). European Association of Urology guidelines on non–muscle-invasive bladder cancer (Ta, T1, and carcinoma in situ). European urology, 81(1), 75-94.
2. Dorafshan, S., Razmi, M., Safaei, S., Gentilin, E., Madjd, Z., & Ghods, R. (2022). Periostin: Biology and function in cancer. *Cancer Cell International, 22*(1), 315. https://doi.org/10.1186/s12935-022-02714-8
3. Kim CJ, Yoshioka N, Tambe Y, Kushima R, Okada Y, Inoue H. Periostin is down-regulated in high grade human bladder cancers and suppresses in vitro cell invasiveness and in vivo metastasis of cancer cells. Int J Cancer. 2005 Oct 20;117(1):51-8. doi: 10.1002/ijc.21120. PMID: 15880581.
4. Litvin J, Selim AH, Montgomery MO, Lehmann K, Rico MC, Devlin H, Bednarik DP, Safadi FF. Expression and function of periostin-isoforms in bone. J Cell Biochem. 2004 Aug 1;92(5):1044-61. doi: 10.1002/jcb.20115. PMID: 15258926.

5. Morra L, Moch H. Periostin expression and epithelial-mesenchymal transition in cancer: a review and an update. Virchows Arch. 2011 Nov;459(5):465-75. doi: 10.1007/s00428-011-1151-5. Epub 2011 Oct 14. PMID: 21997759; PMCID: PMC3205268.
6. Murphy-Ullrich, J. E., & Sage, E. H. (2014). Revisiting the matricellular concept. *Matrix Biology*, *37*, 1–14. https://doi.org/10.1016/j.matbio.2014.07.005
7. Okazaki, T., Tamai, K., Shibuya, R., Nakamura, M., Mochizuki, M., Yamaguchi, K., Abe, J., Takahashi, S., Sato, I., Kudo, A., Okada, Y., & Kennichi Satoh. (2018). Periostin is a negative prognostic factor and promotes cancer cell proliferation in non-small cell lung cancer. *Oncotarget*, *9*(58), 31187–31199. https://doi.org/10.18632/oncotarget.25435
8. Ruan K, Bao S, Ouyang G. The multifaceted role of periostin in tumorigenesis. Cell Mol Life Sci. (2009) Jul;66(14):2219-30. doi: 10.1007/s00018-009-0013-7. Epub 2009 Mar 24. PMID: 19308325.
9. Saginala, K., Barsouk, A., Aluru, J. S., Rawla, P., Padala, S. A., & Barsouk, A. (2020). Epidemiology of bladder cancer. *Medical sciences*, *8*(1), 15.
10. Silvers CR, Liu YR, Wu CH, Miyamoto H, Messing EM, Lee YF. Identification of extracellular vesicle-borne periostin as a feature of muscle-invasive bladder cancer. Oncotarget. (2016) Apr 26;7(17):23335-45. doi: 10.18632/oncotarget.8024. PMID: 26981774; PMCID: PMC5029630.
11. Sung H, Ferlay J, Siegel RL, Laversanne M, Soerjomataram I, Jemal A, Bray F. Global Cancer Statistics 2020: GLOBOCAN Estimates of Incidence and Mortality Worldwide for 36 Cancers in 185 Countries. CA Cancer J Clin. 2021 May;71(3):209-249. doi: 10.3322/caac.21660. Epub 2021 Feb 4. PMID: 33538338

12. Xu, C., Wang, Z., Zhang, L., Feng, Y., Lv, J., Wu, Z., Yang, R., Wu, T., Li, J., Zhou, R., Tian, Z., Bai, J., Zhang, H., Lan, Y., Lv, Z. (2022). Periostin promotes the proliferation and metastasis of osteosarcoma by increasing cell survival and activates the PI3K/Akt pathway. *Cancer Cell International, 22*(1), 34. https://doi.org/10.1186/s12935-021-02441-6